research article

INFLUENCE OF FINISH LINE IN THE DISTRIBUTION OF STRESS TROUGH AN ALL CERAMIC IMPLANT-SUPPORTED CROWN. A 3D FINITE ELEMENT ANALYSIS.

G. SANNINO, F. GLORIA, L. OTTRIA, A. BARLATTANI

University of Rome "Tor Vergata", Department of Odontostomatological Science

SUMMARY

Influence of finish line in the distribution of stress through an all ceramic implant-supported crown. A 3D Finite Element Analysis

Porpose. The aim of this study was to evaluate, by finite element analysis (FEA), the influence of finish line on stress distribution and resistance to the loads of a ZrO_2 crown and porcelain in implant-supported.
Material and methods. The object of this analysis consisted of a fixture, an abutment, a passing screw, a layer of cement, a framework crown, a feldspatic porcelain veneering. The abutment's marginal design was used in 3 different types of preparation: feather edge, slight chamfer and 50°, each of them was of 1 mm depth over the entire circumference. The ZrO_2 Y-TZP coping was 0.6 mm thick. Two material matching for the abutment and the framework was used for the simulations: ZrO_2 framework and ZrO_2 abutment, ZrO_2 framework and T abutment. A 600 N axial force distributed over the entire surface of the crown was applied. The numerical simulations with finite elements were used to verify the different distribution of equivalent von Mises stress for three different geometries of abutment and framework.
Results. Slight chamfer on the matching ZrO_2 - ZrO_2 is the geometry with minimum equivalent stress of von Mises. Even for T abutment and ZrO_2 framework slight chamfer is the best configuration to minimize the localized stress. Geometry that has the highest average stress is one with abutment at 50°, we see a downward trend for all three configurations using only zirconium for both components.
Conclusions. Finite element analysis. performed for the manifacturing of implant-supported crown, gives exact geometric guide lines about the choice of chamfer preparation, while the analysis of other marginal geometries suggests a possible improved behavior of the mating between ZrO_2 abutment and ZrO_2 coping. for three different geometries of the abutment and the coping.

Key words: zirconium dioxide, finite element method, implant supported restoration, marginal design.

RIASSUNTO

Influenza della linea di finitura marginale nella distribuzione degli stress attraverso una corona in ceramica integrale implanto-supportata. Analisi agli elementi finiti

Scopo del lavoro. Lo scopo di questo studio è stato quello di valutare, mediante l'analisi agli elementi finiti, la distribuzione degli stress e la resistenza ai carichi di una corona in ZrO_2 e porcellana implanto-supportata, in funzione di diverse tipologie di disegno marginale dell'abutment.
Materiali e metodi. L'oggetto della presente analisi era costituito dalle seguenti parti: una fixture, un abutment, una vite passante, uno strato di cemento, un coping, un rivestimento estetico in porcellana. Il modello di abutment utilizzato presentava 3 diverse tipologie di preparazione per la configurazione marginale dell'elemento: *feather edge, chamfer* leggero e 50°, ognuna della profondità di 1 mm su tutta la circonferenza. Il coping di ZrO_2 Y-TZP aveva uno spessore calibrato di 0,6 mm. Per abutment e coping si sono utilizzati due diversi accoppiamenti di materiali per le simulazioni: ZrO_2 per entrambi, ZrO_2 per la cappetta e titanio per l'abutment. Si è effettuata una analisi di tipo statico-strutturale applicando una forza pari a 600 N. Le simulazioni numeriche agli elementi finiti sono state usate per verificare la diversa distribuzione degli stress equivalenti di von Mises
Risultati. La geometria che presenta il minimo stress equivalente di von Mises è il chamfer leggero per l'accoppiamento ZrO_2 - ZrO_2.
Anche per abutment in T e coping in ZrO_2 la migliore configurazione per minimizzare gli stress localizzati è il chamfer leggero. La geometria che presenta lo stress medio più elevato risulta essere quella con abutment a 50°, si nota inoltre una tendenza alla diminuzione per tutte e tre le configurazioni utilizzando solo zirconio per entrambi i componenti.
Conclusioni. L'analisi F.E.M. eseguita per la realizzazione di una corona implanto-supportata, dà indicazioni geometriche precise riguardo la scelta della preparazione a chamfer, mentre l'analisi delle altre geometrie marginali suggerisce un possibile miglior comportamento dell'accoppiamento fra abutment e coping in ZrO_2. per tre differenti geometrie di abutment e relativi coping.

Parole chiave: diossido di zirconio, metodo degli elementi finiti, corona implanto supportata, disegno marginale.

Introduzione

Single tooth replacement by an implant supported crown has now become a routine operation for most clinicians.
Several retrospective studies conducted on patients treated with implant supported FPD at 5 and 10 years, showed how to reach a large predictability of treatment, confirmed by the cumulative rate of success with values ranging from 96% to 98% (1, 2).
Today clinicians must reach successful long-term organic – functional score, but at the same time they must satisfy the increasing demands by the patient for work of high aesthetic value.
While Titanium (T) has long been the traditional material for the manufacture of implant abutment for its mechanical properties (3, 4), research has failed to meet these needs by offering high strength ceramic materials as the partially stabilized zirconia (ZrO_2) (5, 6, 7).
These innovative materials require processing by CAD-CAM technologies and are suitable for the realization of both the implant abutment and the crown, giving, thanks to their physical properties – mechanical, natural tooth like color, high load resistance, a 'high biocompatibility with the peri implant tissues and improved intrasulcular adaptability compared to metals commonly used in prosthetic practice (8, 9, 10, 11).
Oxide ceramics are equal to metals from a mechanical standpoint, but are biologically stronger. However, one exception is the high brittleness of ceramics and their potential crack. So far, the use of full – ceramic implant abutments for implant restorations has been limited because of this feature (12, 13, 14, 15 ,16).
Zirconia has mechanical properties similar to those of stainless steel. Its resistance to traction can be as high as 900–1200 MPa and its compression resistance is about 2000 Mpa (5).
Butz et al. evaluated the survival rate, fracture strength, and failure mode of this kind of abutment and found that after chewing simulation and fracture loading, ZrO_2 abutments were comparable to titanium ones (281 N as opposed to 305 N). Also, the fracture rate of zirconia abutments was similar to that of their titanium counterparts (17).
The restoration of ceramic abutments with allceramic crown systems has been described in the literature (18, 19, 20, 21).
There are several ceramic materials for the manifacturing of metal-free restorations using different CAD-CAM systems.
CAD/CAM technology relies on exact dimensional predictions to compensate for sintering shrinkage (22), and is an economical and highly reproducible method for manufacturing complex and individual geometries out of a green or presintered ceramic material (23).
Luthy measured average load-bearing capacities of 518 N for alumina restorations, 282 N for lithium disilicate restorations, and 755 N for zirconia restorations (24).
The bending strength of Yttria stabilized tetragonal Zirconia (Y-TPZ) ceramics is close to the actually used gold alloys (27).
Analyzing different all-ceramic systems, Raigrodski concluded that reinforced ceramics can only be used to replace anterior teeth with single crown restorations or maximum with three units FPDs (22).
On the contrary, Zr-ceramic FPDs can also be used on molars.
Single tooth restorations and fixed partial dentures with a single pontic element are possible on both anterior and posterior elements because of mechanical properties of this material (28, 29, 30).
However, all-ceramic restorations, particularly when placed in the posterior region, which are subjected to stronger forces than anterior, have a history of being prone to brittle fracture (31).
On the other hand, in each of these tests it was demonstrated that zirconia restorations yield superior results in terms of fracture resistance as compared with alumina or lithium disilicate ceramic restorations.
However, the stresses in the veneering porcelain could still determine the longevity (32).
15 studies have demonstrated a 90% or greater success rate using zirconia-based prostheses, and failures were attributed to cracking or crazing of the veneering porcelain (33, 34).
Comparing different core designs a higher fracture strength was found when ZrO_2 core thickness is optimized in order to obtain a uniform thickness of veneer ceramic (35).
Tinschert et al. reported a fracture load for ZrO_2 of

over 2000 N, Sundh et al. measured fracture loads in the range 2700–4100 N, whereas Luthy et al. asserted that a zirconia core could fracture under a load of 706 N (24).
Numerous studies have reported superior fracture strength and toughness data for TZP (26, 33, 36, 37). Anyway clinical success of zirconia based posterior prostheses reaffirms the structural potential of this material (33).
The superior mechanical properties of zirconia allow clinicians to reconsider established preparation guidelines for the design and consider important variations such as reducing the coping thickness from 0.5 mm to 0.3 mm and changing finish line preparations from chamfer (CHA) to minimally invasive knifeedge (KNE) margins.
In vitro research evaluating the influence of processing variables on fracture resistance of all-ceramic restorations has revealed highly divergent failure loads of 450 to 1600 N for zirconia single crown copings, depending on coping thickness, design of finish line, and applied luting agent (30, 38, 39).
In general, higher fracture loads can be produced by increasing the coping thickness or by using adhesive luting materials instead of retentive cementation (40, 41, 42).
However, conventional cementation is recommended by the manufacturers.
An other influence on fracture resistance is the design of the finish line (43).
For all-ceramic restorations, the CHA and shoulder preparation are recommended.
These finish line configurations are reported to transfer a minimum of masticatory stress from the coping into the veneering porcelain.
In contrast, more conservative preparations, such as feather edge, provide the most acute marginal finish line and allows the clinician to preserve a maximum of sound tissue to prevent tooth weakening or pulp irritation, due to the heat generated by cutting action of the cutters (44).
As a consequence, restoration dimensions with reduced coping thicknesses or less invasive finish lines, including KNE, are needed, particularly for lingual surfaces of mandibular posterior teeth, for teeth with convex axial surfaces, and for inclined tooth surfaces.
Howewer for prosthetic rehabilitation which use both natural teeth and implant abutment research has always been tested type and predictability of the design of finish line (33, 44, 48).
Today in the middle of implant age, for the manifacturing of an optimal implant supported crown, researcher try to define what might be best material and configuration which it could and / or should be used with. That's to achieve success in terms of reliability, depending on the clinical situation of our rehabilitation.
The FEM (finite element method)seems to be a proper tool to study material behavior in relation to their composition, inter - relationship and geometry, by analyzing the distribution of stress.
The FEM acronym is derived from finite element method, whereas FEA, from Finite element analysis, is the real finite element analysis.
Known since the'50s, the finite element method has spread only much later. Today, thanks to the availability of high-performance computers, has become one of several methods of calculation used in all branches of engineering, from structural analysis to the computational fluid dynamics (CFD).
It's a mathematical method for the differential equations resolution. We can describe the behavior of different structures using of differential equations: the equation relating to the elasticity theory resolution allows, for example, to study the behavior of a solid body, as an implant-supported crown or bridge under the influence of different loads and thus calculate stresses and deformations. In simple cases differential equations resolution can be done analytically, but in the case of more complex and discontinuous systems, which normally occur in practice, this becomes impossible. For this reason, mathematical approaches that allows to use a numerical approximation is the most suitable. Among these, a method is particularly effective: the finite element method (FEM or, from Finite Element Method). This mathematical method started with the mathematical Ritz and Courant. Their idea was to describe the global behavior of a complex system combining several simple parametric functions, each representative of a portion of the system. Therefore, the differential equation solution is nothing else than the resolution of the unknows of a system of easier algebraic equations.
The unknowns could be, depending on the situation, a shift, a temperature or a magnetic potential. For complex structures algebraic equation systems

can become huge with an infinite number of unknowns to be calculated. Therefore the FEM calculation development occurred only when the computers achieved an adequate power calculation.
In the'70s, the FEM calculations were performed only in large companies or in computer centers by highly specialized personnel. At that time, available software required huge machines for the operation, called "mainframes", that only few companies could afford.
Nowadays, by much more powerful computers than in the past, we can develop more complex models in less time. Thanks also to the now available graphical user interfaces, we can prepare a model and obtain results saving time and money. Since the modeling phase is still the longest stage of the calculation method, we try, increasingly, to start directly from geometric models produced by CAD.
The finite element method calculation allows today to answer several questions in the field of static, dynamic, electromagnetism, physics of fluids, of sound and in cases where different fields of physics are associated with each other such as in the case of piezoelectricity. Imagine an implant supported crownet will bear the load chewing? It will also withstand the loads resulting from eccentric movements parafunctional (bruxismo)?
What is the influence of a change in a geometric construction? To all these questions and situations, the FEM calculation may provide an answer. The finite element method is a powerful available tool for a reasonable cost.
The planning stage of a product can represent up to 75% of the cost of its manufacture.
Product development process presents a huge potential for competitive companies.
Products can be studied and optimized from the design stage up to their effective manifacturing by finite element method.
In this way both the design time and the prototype number can be reduced. The FEM also allows to save resources and gain innovative products with better quality.
The finite element method is not only a useful tool in the automotive, aeronautical and construction but can also be used in the development, construction and research stages across all industry sectors such as in nanotecnic (MEMS) or in biomedical.
We can know what stress distribution through the structure will be and to know in advance how the material will react to these stress according to their mechanical properties by fem analysis.
Finite element method main feature is the discretization of the starting continuous domain in a discrete domain (mesh) using simple shape (triangles and quadrilaterals in 2D domains, esaedri and tetrahedra for 3D domains) primitives (finite elements) linked together by nodes, describing in this way, the global stiffness matrix given by the stiffness matrics of each element that constitutes the model. Each element is featured by elemental form, the solution is assumed to be expressed by linear combination of functions called basic functions or functions of form (shape functions). The function is approximated, and exact function values not necessarily will be those calculated in points, but the values that provide the least error over the entire solution.
A variety of specializations under the umbrella of the mechanical engineering discipline (such as aeronautical, biomechanical, and automotive industries) commonly use integrated FEM in design and development of their products. Several modern FEM packages include specific components such as thermal, electromagnetic, fluid, and structural working environments. In a structural simulation, FEM helps tremendously in producing stiffness and strength visualizations and also in minimizing weight, materials, and costs.
FEM allows detailed visualization of where structures bend or twist, and indicates the distribution of stresses and displacements. FEM software provides a wide range of simulation options for controlling the complexity of both modeling and analysis of a system. Similarly, the desired level of accuracy required and associated computational time requirements can be managed simultaneously to address most engineering applications. FEM allows entire designs to be constructed, refined, and optimized before the design is manufactured.
This powerful design tool has significantly improved both the standard of engineering designs and the methodology of the design process in many industrial applications. The introduction of FEM has substantially decreased the time to take products from concept to the production line. It is primarily through improved initial prototype designs using FEM that testing and development have been accelerated. In summary, benefits of FEM include increased accura-

cy, enhanced design and better insight into critical design parameters, virtual prototyping, fewer hardware prototypes, a faster and less expensive design cycle, increased productivity, and increased revenue. FEA was originally developed in the aircraft industry and has become widespread in the engineering field.
In dentistry, FEA has been used to determine stress distributions in teeth, implants and various restorations under occlusal static and dinamic forces by authors like Farah, Anusavice, DeHoff, Hojjatie, Palmara, Kamposiora, etc.
The aim of this study was to evaluate, by finite element analysis (FEA), the influence of finish line on stress distribution and resistance to the loads of a ZrO_2 crown and porcelain in implant-supported.

Material and methods

The geometry for the designs was obtained from 2D drawings of components provided by the implant manufacturer (BTLock srl, Vicenza, Italy) The model was created in 3D using the solid modeling software (Solidworks office 2007, Solidworks Corporation).
The object consisted of:
- fixture
- abutment

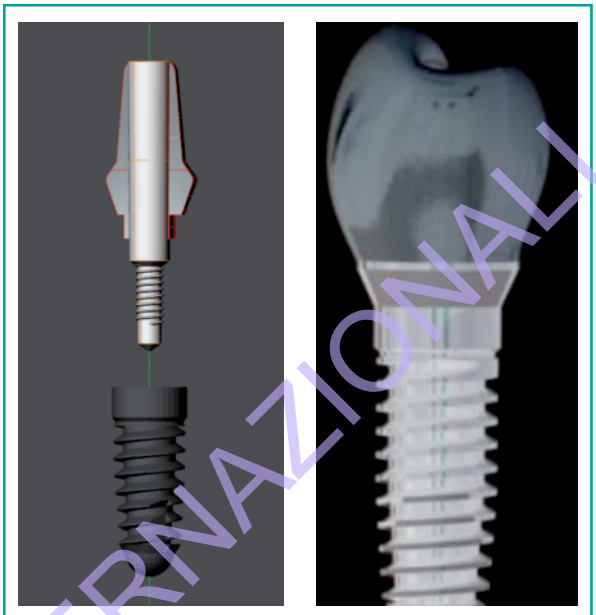

Figure 1
Graphical representation of model parties.

- passing screw- layer of cement
- framework crown
- feldspatic porcelain veneering

as shown in Figure 1:
A fixture 4.50x13-mm (BT-TITE One Line, 45013 BTICV1, BTLock srl, Vicenza, Italy) was selected for this study.

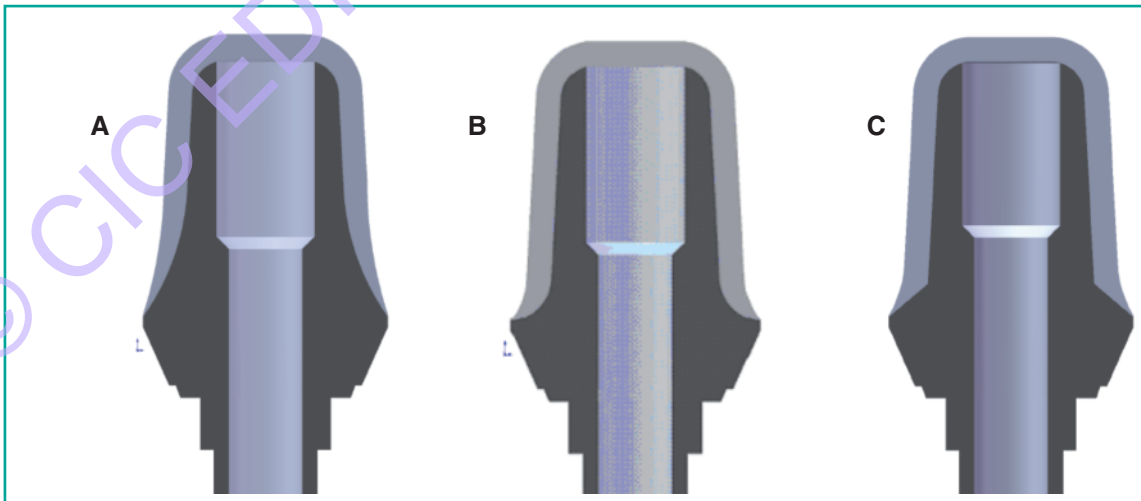

Figure 2
A - Feather edge; B - Chamfer; C - 50°.

It was realized by a revolution along the symmetry axis of a sketch on the plan, the external and internal threads were obtained using a sweep around a spiral propeller on the longitudinal axis of the fixture.
The abutment choosen (Abutment Shoulder, 450B BTIPMLS, BTLock srl) was realized in 3D through a process of revolution along the longitudinal axis too. It had a minor diameter of 4.70 in the coupling with the fixture, a major diameter greater of 6 mm in the coupling with the crown, a radial shoulder of 0,625 mm depth, a total length of 5.90 mm and an inclination of the axial walls of 3°.
The 3D modeling of the screw passing (Short Through Screw, BTIVPC, BTLock srl) was performed with the same procedure of the fixture.
Most previous publications involving FEA have modeled screw threads and the screw bore using concentric rings because of the difficulty in modeling the thread helix. However, because the abutment screw would be tightened
to induce the preload during the FEA by simulating screwing the abutment screw into the screw bore and clamping the abutment onto the implant, the exact geometry of the thread helix was necessary. A concentric ring cannot be screwed into a screw bore.
The abutment's marginal design was used in 3 different types of preparation: feather edge, slight chamfer and 50°, each of them was of 1 mm depth over the entire circumference (Fig. 2).
A slight chamfer connecting the occlusal surface and the axial wall was also made.
A 0,025 mm thick layer of adhesive resin permanent, dual double-paste, cement (RelyX ARC, Dental Laboratory Products, St. Paul, Minnesota, USA) was between abutment and coping. The ZrO_2 Y-TZP coping (Copran, White Peaks Dental GmbH & Co. KG, Essen, Germany) was 0.6 mm thick.
A first right mandibular premolar feldspatic veneering porcelain (Noritake Dental Supply Co., Limited, Japan) was modeled on the coping by a loft function applied to the guidelines made by spline.
All materials used were assumed to be linearly elastic, homogeneous and isotropic.
The mechanical properties were data supplied by the manufacturers and are showed in Table 1.
The fixture and the passing screw were made of T,
The simulated crown consisted of framework material and porcelain.

Table 1 - Mechanical properties of different materials.

Material	Elastic module [GPa]	Poisson Coeff.
Titanium	110	0,34
Cement	5,1	0,27
Zirconium	210	0,3
Porcelain	70	0,25

the Y- TZP ZO_2 was used as the crown framework material and feldspathic porcelain was used for the occlusal surface; a thin cement layer linked framework to the abutment.
Two material matching for the abutment and the framework was used for the simulations:
- ZrO_2 framework and ZrO_2 abutment
- ZrO_2 framework and T abutment.
In this way within the three different geometries was also evaluated the best material matching.
Thus the model was imported for finite aelement analysis in the FEM calculation software ANSYS 1.1 (ANSYS Inc., Canonsburg, Pennsylvania, USA), using the following modules:
- by pre-processor about the problem were included data (geometry, characteristic of the material, model discretization, assignment constraints and loads);
- by solver analysis was set and solved;
- by postprocessor results were shown

Modeling of the problem

Importing CAD geometry, which was composed in several parts, various components were bound to simulate real interface between the parts and make the analysis of the system as a whole.
From knowledge of the physics of the problem, connections between the different parts can be defined by choosing one of the possible types of constraints described below and illustrated in Table 2:
- Bonded (bound): constraint on both normal (bilateral) and tangential, it is set by default, it determines the bonding of two sides in contact.
- Without separation (no separation): constraints only normal (bilateral), but not tangential, it not allows to regions to separate themeselves.
- Frictionless (no friction): constraints only normal (unilateral), but not tangential, it allows both the

Table 2 - Interface Type.

NAME	Separation	Flow	Type of analysis
Bonded	No	No	Linear
Rough	Yes	Infinite	Non linear
No separation	No	Yes	Linear
Frictionless	Yes	Yes	Non linear
Frictional	Yes	Yes	Non linear

slider and the creation of gaps between the interfaces.
Rough-(roughness): constraint on both normal (unilateral) or bypass, it allows the separation of interfaces but does not allow scrolling (coefficient of friction infinity).
Frictional (with friction): constraint on both normal (unilateral) and tangential to the limit of friction that is set in the analysis.
Below you can see a description of the bond used for the interface between the various components:

1. veneeringporcelain - framework: bound
2nd framework - cement: bound
3rd Cement-abutment: bound
4th passing screw - abutment: no separation
5th fixture – passing screw: bound
6th fixture - abutment without separation

The logic with which they were selected interfaces is as follows: parts between them that allow the slider (for example screw fasteners and internal abutment) were associated with the bond without separation while those stuck with the bond is normal for tangential (bonded).
The mesh of the analysis consists of SOLID187 elements, three-dimensional elements formed from 10 knots and very suitable for developing mesh on irregular bodies (as the crown is).
The SOLID187 can solve problems dealing with plasticity, iperplasticity, creep, large deflection and substantial stress and allows to make structural analysis.
A static-structural analysis was performed to study the linear elastic materials behavior (elastic modulus and Poisson ratio for the tests was sufficient). The purpose of the study was to verify stress distribution within the components of the system and so a 600 N axial force distributed over the entire surface of the crown was applied to avoid localized stress.
In Figure 3 shows the crown area where the force with its direction was applied (the force has the negative direction of axis y).
The decision to place the load distributed across the crown instead of using individual concentrated forces was carried out to prevent the emergence of concentrations of stress that are not realistic to simulate the phenomenon of chewing.
In fact, the contact of food with the crown causes a redistribution of power on most of the occlusal surface of the crown, simulating a pad that redistributes force on a wider area.
This choice was made for a better graphical representation of stress shown on the post-processor, as a force localized on a single node would have significantly expanded the stress scale.
A fixed constraint on the external thread was ap-

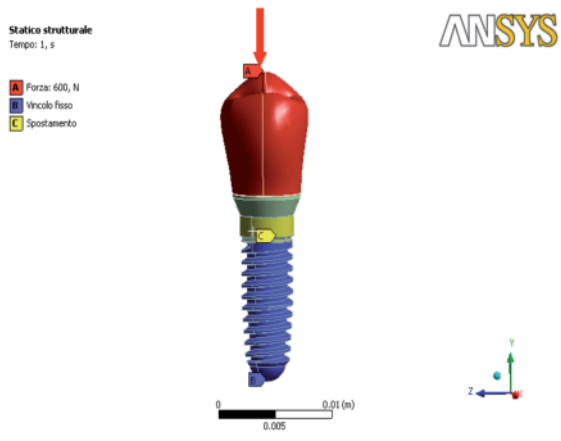

Figure 3
Loads and constraints applied.

plied, while non-threaded portion was bound only in the xz directions to allow tangential movement in the bone to simulate the joints in mandibular bone.
The numerical simulations with finite elements were used to verify the different distribution of equivalent von Mises stress for three different geometries of abutment and framework.
For each of the individual simulations was carried out an analysis of convergence of the mesh on the framework (which is the subject of comparison), this to reach the peak value of voltage through successive refinements with a change to more than 5%.

Results and discussions

Graphic 1 describes the analysis of convergence of the maximum voltage on the number of nodes used in the mesh.
For different different types of mesh tests were used, illustrated in Figure 4, duly finished in matching areas of greatest concentration of stress.
Table 3 shows the parameters of the three different *mesh* used.
The solutions were obtained by trying to remove any postings and interpenetration between the finite elements which constitute the numerical model, due to imperfect matching of the elements gained from the discretization of the tested areas.
These intermingling are the cause of the peak voltage positions located in very restricted geometry.
Therefore it is useful to perform as well as a comparison of the maximum peak voltage in geometry even a comparison between the average distributions of tensions.
The following images show a distinction between what the average equivalent stress is (the distribution) and localized peaks of tension that are mostly due to the units to contact discretization.
Figure 5 shows stress distribution of throughout the model, the maximum value corresponding to 92 MPa is obtained where the thread starts (the first portion of thread is what first must resist the applied load).

Table 3 - Mesh Parameters.

Geometry	Elements N°	Nodes N°
Slight Chamfer	94497	165582
50°	97706	170855
Feather Edge	88904	156291

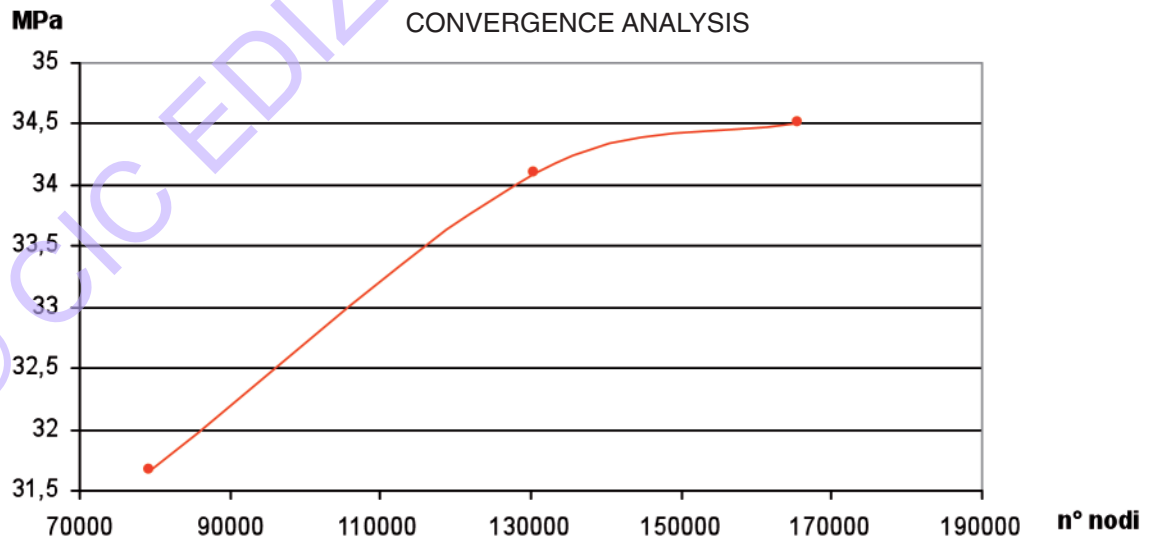

Graphic 1
Convergence of analysis of the mesh.

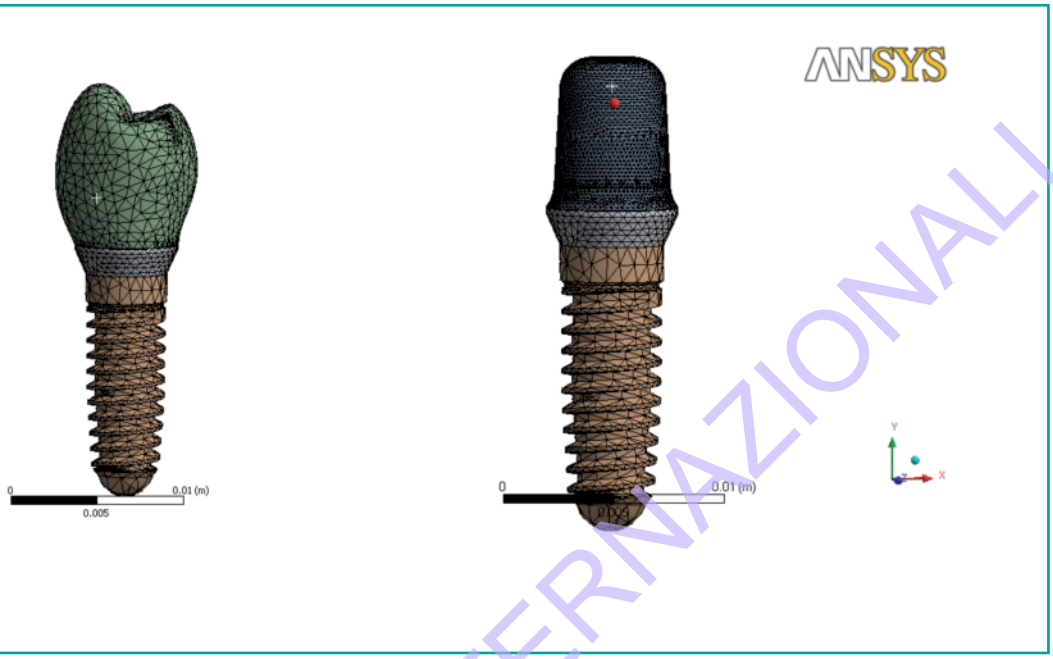

Figure 4
Mesh used.

In this analysis comparison of the stresses on the different configurations of abutment and framework is important and so the maximum values obtained on the thread will be forgot.
Table 4, and thereafter as graphic 2, shows the values of the peak voltage recorded for the three geometries and two different matching of materials for abutment and framework.
Slight chamfer on the matching ZrO_2 - ZrO_2 is the geometry with minimum equivalent stress of von Mises.
Even for T abutment and ZrO_2 framework slight chamfer is the best configuration to minimize the localized stress.
Individual nodes of the geometric framework discretization (65.535 nodes) voltage values were exported from ANSYS to make a comparison on the medium voltage distribution on framework in the three different configurations and for two different materials and the arithmetic mean to obtain the results shown in Table 5 and in the graphic 3 was conducted.
Even from these values we see that the best compromise you get with the configuration with slight chamfer abutment and coping in zirconium.
Geometry that has the highest average stress is one with abutment at 50°, we see a downward trend for all three configurations using only zirconium for both components.
Figure 6 shows the equivalent von Mises stress

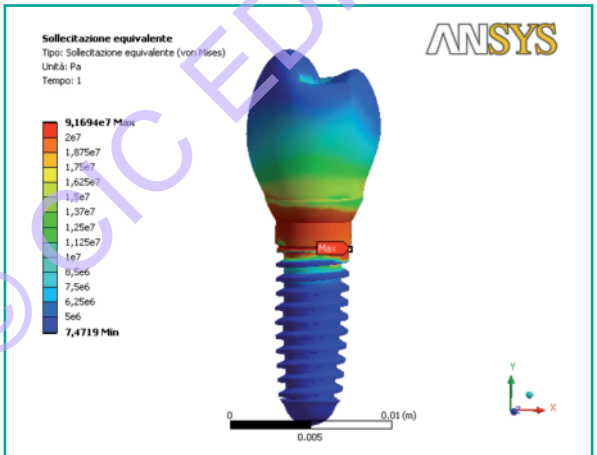

Figure 5
Distribution of stress trough the complete model.

Table 4 - Maximum stress for different configurations.

	ZrO_2-T [MPa]	ZrO_2- ZrO_2 [MPa]
Slight Chamfer	34,5	30
50°	37,4	34,9
Feather Edge	41,5	32

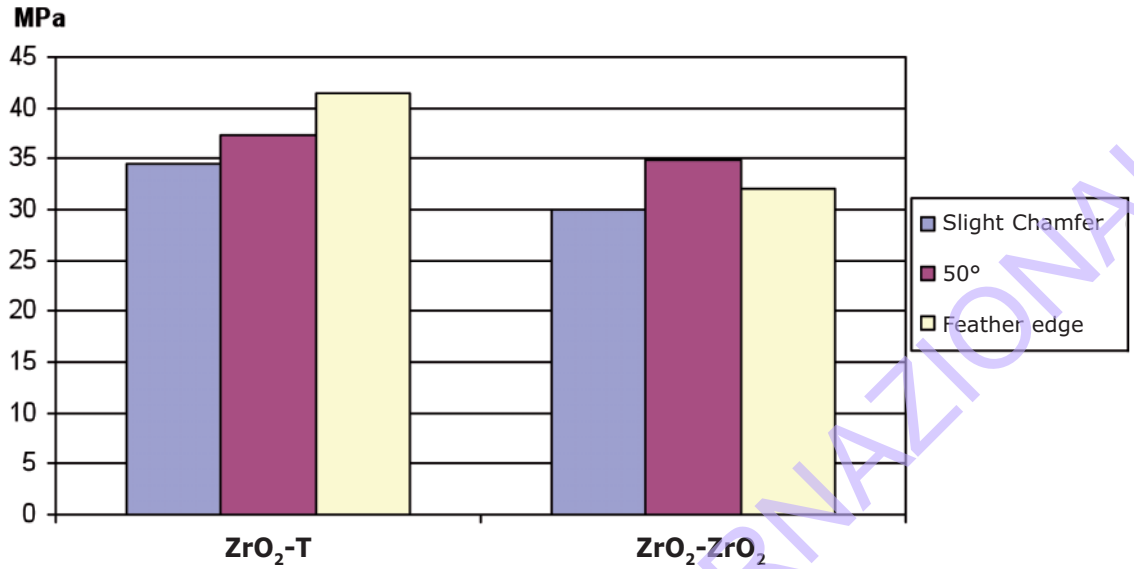

Graphic 2
Comparison of maximum tension.

distribution, the colors are as indicated in the scale shown to the side.
The maximum stress values are indicated by orange and correspond on an average of 20 MPa

Table 5 - Stress avarage for the different configurations.

	ZrO_2-T [MPa]	ZrO_2-ZrO_2 [MPa]
Slight Chamfer	11,18	11,17
Abutment 50°	15,7	14,2
Feather edge	15,5	13,7

while the minimum values are indicated by blue and are lower than 5 Mpa.
As you can see for each of 3 different geometries, the minimum stress is localized in a circular area on top of framework, because in this area the framework is not compressed against the abutment due to the hole of the passing screw.
The base junction is the region with the largest stress values, infact in this area there are compression and cutting stresses.
The following image (Figure 7) shows that using only ZrO_2 stress distribution presents scales lower (yellow and green area are wider than orange one).
Figure 8 and Figure 9 show images of the 50° configuration abutment, in the blue labels maximum and minimum values recorded by the "probe" available in ANSYS are measured.
The maximum values are higher than those obtained by chamfer geometry and in this case, the stress went down using ZrO_2 for both components.
Figure 10 and Figure 11 show the results obtained

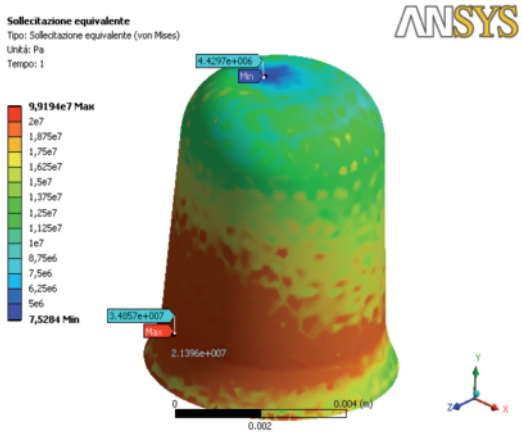

Figure 6
Slight chamfer (ZrO_2 framework- T *abutment*).

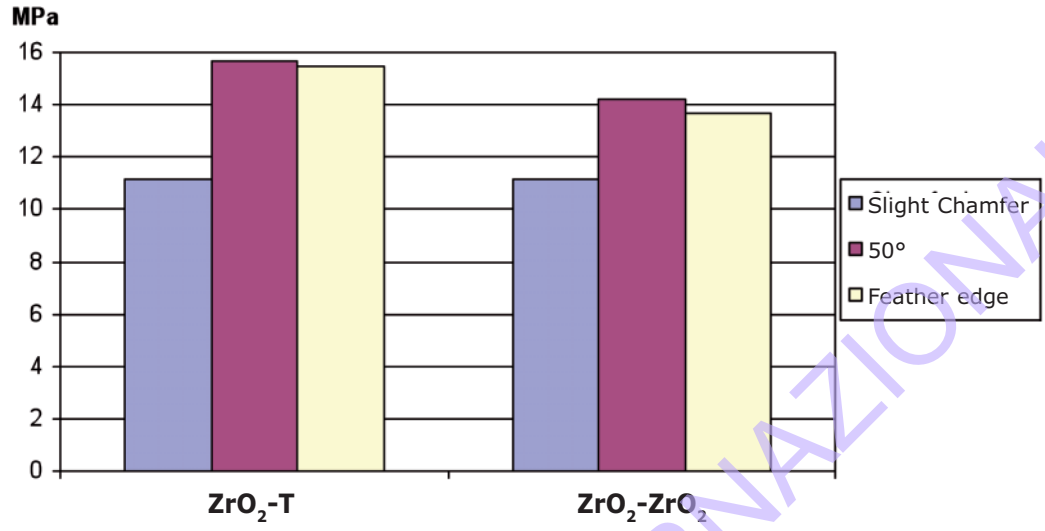

Graphic 3
Comparison of mediated tensions.

for the feather edge model, in this case with the titanium abutment stress concentrated are higher than the other two configurations, while the average value is lower than the 50° configuration.
In this work a numerical model for finite element analysis of mechanical behavior of prosthetic components used in the implants trethments is showed.
After an initial study phase of the model and the interaction of the various parts (units with complex geometric shapes and different materials), the discretization analysis of the numerical model was carried out, defining the contour conditions to get the same geometric configurations and loads that the real model in its typical configuration of "work" would have.
The numerical predictions of the model generated in this way, have been shown in good agreement with experimental and theoretical results obtained from the literature.

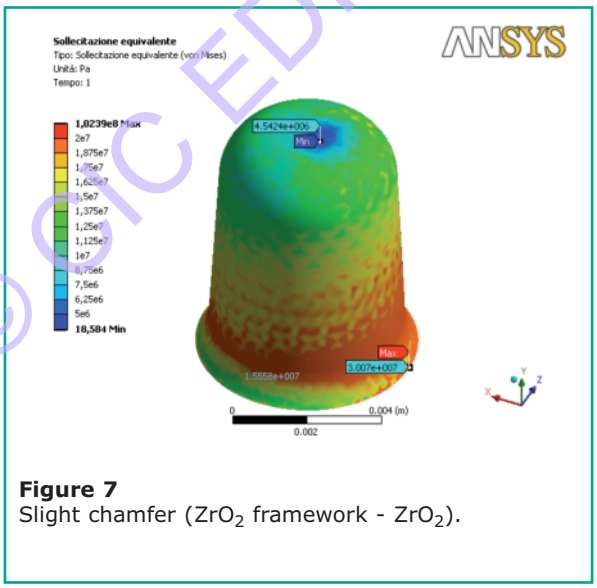

Figure 7
Slight chamfer (ZrO_2 framework - ZrO_2).

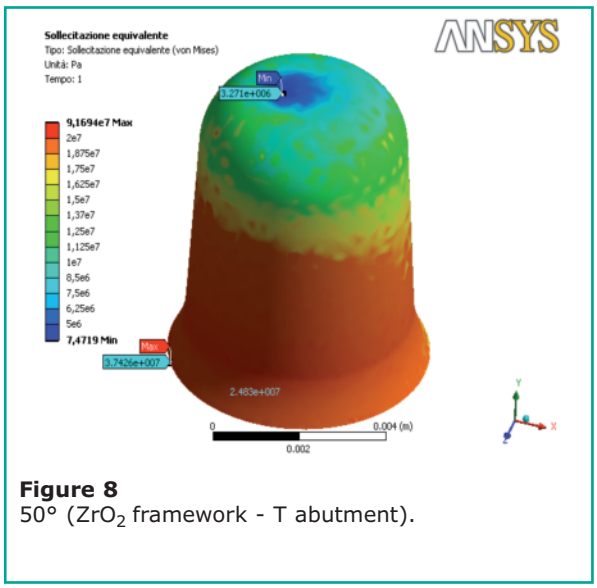

Figure 8
50° (ZrO_2 framework - T abutment).

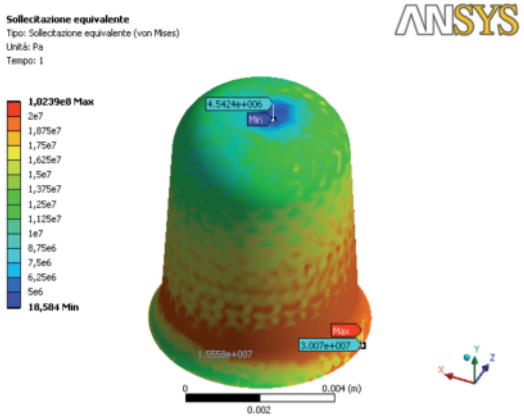

Figure 9
50° (ZrO_2 framework - ZrO_2 abutment).

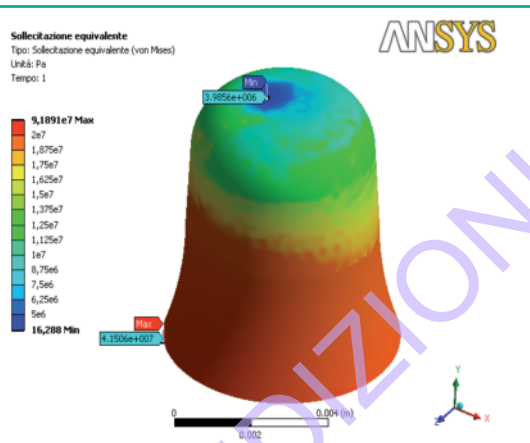

Figure 10
Feather edge (ZrO_2 framework - T abutment).

Conclusion

In respect of the results shown before the slight chamfer with ZrO_2 abutment and ZrO_2 framework could be the best geometry to minimize the stress, while 50° geometry could have a lower performance, in fact, components under loads should have geometries connected as possible to decrease the maximum equivalent stress.

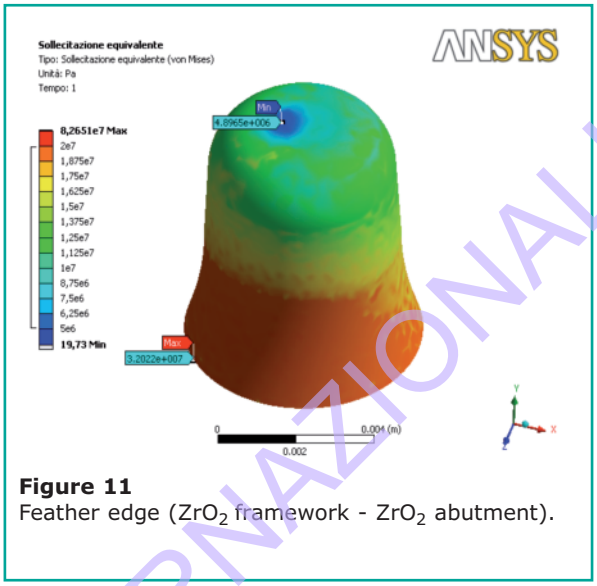

Figure 11
Feather edge (ZrO_2 framework - ZrO_2 abutment).

Sharp edges, inside of components subject to alternating loads, are interested in fractures for fatigue after a number of cycles lower than the same components, but with a larger radius of curvature, and this is for the effect of tensional concentration. With this observation, we can say that a prosthesis, because continuously under alternating loads due to chewing, has a greater fatigue life if he has more extensive connections.
There is also a tendency as in the average values even in the peak voltage to a stress reduction on framework using ZrO_2 as material for both units.

References

1. Andersson B, Ödman P, Lindvall A-M, Brånemark P-I. Cemented single crowns on osseointegrated implants after 5 years: Results from a prospective study on CeraOne. Int J Prosthodont 1998; 11: 212–218.
2. Scholander S. A retrospective evaluation of 259 single-tooth replacements by the use of Brånemark implants. Int J Prosthodont 1999; 12: 483–491.
3. Christel P, Meunier A, Heller M, Torre JP, Peille CN. Mechanical properties and short-term in-vivo evaluation of yttrium-oxide-partially- stabilized zirconia. J Biomed Mater Res 1989; 23: 45-61.
4. Seghi RR, Denry IL, Rosenstiel SF. Relative fracture toughness and hardness of new dental ceramics. J

Prosthet Dent 1995; 74: 145-50.
5. Piconi C, Maccauro G. Zirconia as a ceramic biomaterial. Biomaterials 1999; 20: 1-25.
6. Avivi-Aber L, Zarb GA. Clinical effectiveness of implant-supported single tooth replacement: The Toronto Study. Int J Oral Maxillofac Implants 1996; 11: 311-321.
7. Scheller H, Kultjr C, Klineberg I, et al. A 5-year multicenter study on implant-supported single crown restorations. Int J Oral Maxillofac Implants. 1998; 13: 212-218.
8. Filser F, Kocher P, Weibel F, Lüthy H, Schärer P, Gauckler LJ. Reliability and strength of all-ceramic dental restorations fabricated by direct ceramic machining (DCM).Int J Comput Dent 2001 Apr; 4 (2): 89-106.
9. Tinschert J, Natt G, Mautsch W, Augthun M, Spiekermann H. Fracture resistance of lithium disilicate-, alumina-, and zirconia-based three-unit fixed partial dentures: a laboratory study.Int J Prosthodont 2001 May-Jun; 14 (3): 231-8.
10. Ichikawa Y, Akagawa Y, Nikai H, Tsuru H. Tissue compatibility and stability of a new zirconia ceramic in vivo. Prosthet Dent. 1992 Aug; 68 (2): 322-6.
11. Döring K, Eisenmann E, Stiller M. Functional and esthetic considerations for single-tooth Ankylos implant-crowns: 8 years of clinical performance. J Oral Implantol. 2004;30(3):198-209.
12. Akagawa Y, Ichikawa Y, Nikai H, Tsuru H. Interface histology of unloaded and early loaded partially stabilized zirconia endosseous implant in initial bone healing. J Prosthet Dent. 1993 Jun; 69 (6): 599-604.
13. Covacci V, Bruzzese N, Maccauro G, Andreassi C, Ricci GA, Piconi C, Marmo E, Burger W, Cittadini A. In vitro evaluation of the mutagenic and carcinogenic power of high purity zirconia ceramic. Biomaterials 1999 Feb; 20 (4): 371-6.
14. Scarano A, Piattelli M, Caputi S, Favero GA, Piattelli A. Bacterial adhesion on commercially pure titanium and zirconium oxide disks: an in vivo human study J Periodontol. 2004 Feb; 75 (2): 292-6.
15. Degidi M, Artese L, Scarano A, Perrotti V, Gehrke P, Piattelli A. Inflammatory infiltrate, microvessel density, nitric oxide synthase expression, vascular endothelial growth factor expression, and proliferative activity in peri-implant soft tissues around titanium and zirconium oxide healing caps. J Periodontol. 2006 Jan; 77 (1): 73-80.
16. Ferrario VF, Sforza C, Serrao G, Dellavia C, Tartaglia GM. Single tooth bite forces in healthy young adults. Oral Rehabil. 2004 Jan; 31(1): 18-22.
17. Butz F, Heydecke G, Okutan M, Strub JR. Survival rate, fracture strength and failure mode of ceramic implant abutments after chewing simulation. Journal of Oral Rehabilitation 2005; 32: 838–43.
18. Glauser R, Sailer I, Wohlwend A, Studer S, Schibli M, Scharer P. Experimental zirconia abutments for implant-supported single-tooth restorations in esthetically demanding regions: 4-year results of a prospective clinical study. Int J Prosthodont 2004; 17: 285-90.
19. Yildirim M, Edelhoff D, Hanisch O, Spiekermann H. Ceramic abutments—a new era in achieving optimal esthetics in implant dentistry. Int J Periodontics Restorative Dent 2000; 20: 81-91.
20. Ottl P, Piwowarczyk A, Lauer HC, Hegenbarth EA. The Procera AllCeram system. Int J Periodontics Restorative Dent 2000; 20: 151-61.
21. Probster L. All-ceramic crowns on modified CeraOne abutments: a case report. Quintessence Int 1998; 29: 52-65.
22. Raigrodski AJ. Contemporary materials and technologies for all-ceramic fixed partial dentures: a review of the literature. Journal of Prosthetic Dentistry 2004; 92: 557–62.
23. Tinschert J, Natt G, Hassenpflug S, Spiekermann H. Status of current CAD/CAM technology in dental medicine. Int J Comput Dent 2004; 7: 25-45.
24. Luthy H, Filser F, Loeffel O, Schumacher M, Gauckler LJ, Hammerle CH. Strength and reliability of four-unit allceramic posterior bridges. Dental Materials 2005; 21: 930–7.
25. Luthardt RG, Holzhu¨ter M, Sandkuhl O, Herold V, Schnapp JD, Kuhlisch E, et al. Reliability and properties of ground Y-TZP-zirconia ceramics. J Dent Res 2002; 81 (7): 487–91.
26. Guazato M, Albakry M, Ringer SP, Swain MV. Strength, fracture toughness and microstructure of a selection of allceramic materials. Part II. Zirconia-based dental ceramics. Dent Mater 2003; 20(5): 449–56.
27. McLean JW. Current status and future of ceramics in dentistry. Eng Sci Ceram Proc 1985; 1–9.
28. Gamb rena I, Blatz MB. A clinical guidelines to predictable esthetics with Zirconium oxide Ceramic restorations. Quintessence of Dental Technology 2006; 29: 11–23.
29. Piwowarczyk A, Ottl P, Lauer HC, Kuretzky T. A clinical report and overview of scientific studies and clinical procedures conducted on the 3M ESPE Lava All-Ceramic System. Journal of Prosthodontic 2005; 14: 39–45.
30. Potiket N, Chiche G, Finger IM. In vitro fracture strength of teeth restored with different all-ceramic crown systems. Journal of Prosthetic Dentistry 2004; 92: 491–5.
31. B. Hojjatiè and K. J. Anusavice three-dimensional finite Element analysis of glass-ceramic dental crowns J. Biomechanics 1990; 23: 1157-1166.
32. De Jager N, Pallav P, Feilzer AJ. The influence of design parameters on the FEA-determined stress distribution in CAD-CAM produced all-ceramic dental crowns. Dent Mater 2005; 21: 242–51.

33. Denry I, Kelly JR. State of the art of zirconia for dental applications. Dent Mater 2007 [Epub ahead of print].
34. Sailer I, Feher A, Filser F, Luthy H, Gauckler LJ, Scharer P, et al. Prospective clinical study of zirconia posterior fixed partial dentures: 3-year follow-up. Quintessenze Int 2006; 37: 685-93.
35. Sundh A, Sjogren G. Fracture resistance of all-ceramic zirconia bridges with differing phase stabilizers and quality of sintering. Dental Materials 2006; 22: 778–84.
36. Claussen N. Microstructural design of zirconia-toughened ceramics (ZTC). In: Claussen N, Ruhle M, Heuer AH, editors. Science and technology of zirconia II, advances in ceramics. Vol 12. Columbus: The American Ceramic Society, Inc; 1984. p. 325-51.
37. Evans AG. Perspective on the development of high-toughness ceramics. J Am Ceram Soc 1990; 73: 187-206.
38. Bindl A, Luthy H, Mormann WH. Thinwall ceramic CAD/CAM crown copings: strength and fracture pattern. J Oral Rehabil 2006; 33: 520-8.
39. Rekow ED, Harsono M, Janal M, Thompson VP, Zhang G. Factorial analysis of variables influencing stress in all-ceramic crowns. Dent Mater 2006; 22: 125-32.
40. Leevailoj C, Platt JA, Cochran MA, Moore BK. In vitro study of fracture incidence and compressive fracture load of all-ceramic crowns cemented with resin-modified glass ionomer and other luting agents. J Prosthet Dent 1998; 80: 699-707.
41. Bernal G, Jones RM, Brown DT, Munoz CA, Goodacre CJ. The effect of finish line form and luting agent on the breaking strength of Dicor crowns. Int J Prosthodont 1993; 6: 286-90.
42. Ernst CP, Cohnen U, Stender E, Willershausen B. In vitro retentive strength of zirconium oxide ceramic crowns using different luting agents. J Prosthet Dent 2005; 93: 551-8.
43. Proos KA, Swain MV, Ironside J, Steven GP. Influence of core thickness on a restored crown of a first premolar using finite element analysis. Int J Prosthodont 2003; 16: 474-80.
44. Shillingburg HT, Hobo S, Whitsett LD, Jacobi R, Brackett SE. Principles of tooth preparation. In: Fundamentals of fixed prosthodontics. 3rd ed. Chicago: Quintessence 1997; p. 119-37.
45. Vult von Steyern P, Carlson P, Nilner K. All-ceramic fixed partial dentures designed according to the DC-Zirkon technique. A 2-year clinical study. J Oral Rehabil 2005; 32: 180-7.
46. Kelly JR. Clinically relevant approach to failure testing of all-ceramic restorations. J Prosthet Dent 1999; 81: 652-61.
47. Lawn BR, Pajares A, Zhang Y, Deng Y, Polack MA, Lloyd IK, Rekow ED, Thompson VP. Materials design in the performance of all-ceramic crowns. Biomaterials 2004; 25: 2885-92.
48. Sorensen JA, Engelman MJ. Ferrule design and fracture resistance of endodontically treated teeth. J Prosthet Dent 1990; 63: 529- 36.

Correspondence to:
Dr. Gianpaolo Sannino
Department of Odontostomatological Science
School of Dentistry.
University of Roma "Tor Vergata"
Via Montpellier, 1 - 00133 Roma
E-mail: gianpaolosannino@uniroma2.it